Selective Observation of Charge Storing Ions in Supercapacitor Electrode Materials

Alexander C. Forse[a,b], John M. Griffin[a,c], and Clare P. Grey[a*]

[a]*Department of Chemistry, University of Cambridge, Lensfield Road, Cambridge, CB2 1EW, U.K.*
[b]*Current address: Department of Chemistry, Department of Chemical and Biomolecular Engineering, and Berkeley Energy and Climate Institute, University of California, Berkeley, California 94720, U.S.A.*
[c]*Current address: Department of Chemistry and Materials Science Institute, Lancaster University, Lancaster LA1 4YB, U.K.*

*Corresponding author. Email: cpg27@cam.ac.uk

Abstract: Nuclear magnetic resonance (NMR) spectroscopy has emerged as a useful technique for probing the structure and dynamics of the electrode-electrolyte interface in supercapacitors, as ions inside the pores of the carbon electrodes can be studied separately from bulk electrolyte. However, in some cases spectral resolution can limit the information that can be obtained. In this study we address this issue by showing how cross polarisation (CP) NMR experiments can be used to selectively observe the in-pore ions in supercapacitor electrode materials. We do this by transferring magnetisation from ^{13}C nuclei in porous carbons to nearby nuclei in the cations (^{1}H) or anions (^{19}F) of an ionic liquid. Two-dimensional NMR experiments and CP kinetics measurements confirm that in-pore ions are located within Ångströms of sp^2-hybridised carbon surfaces. Multinuclear NMR experiments hold promise for future NMR studies of supercapacitor systems where spectral resolution is limited.

1. Introduction

Supercapacitors are high power energy storage devices that store charge at the interface between porous carbon electrodes and an electrolyte solution. While they can charge and discharge much more quickly than batteries, their energy densities are considerably lower, prompting research into the molecular mechanisms of charge storage.[1,2] Molecular simulations,[3–7] and more recently *in situ* characterisation methods,[8–21] have been developed to study supercapacitor charging mechanisms. Together these studies have shown that charging is generally more complex than a simple ion adsorption driven process, and often involves the swapping of counter-ions and co-ions. Very recently molecular simulations have also been used to study the dynamic properties of the electrode-electrolyte interface in supercapacitors,[5,22–24] but experimental validation of the findings of these studies is still limited.

Nuclear magnetic resonance (NMR) spectroscopy is emerging as a promising experimental tool to probe the structure and dynamics of the electrode-electrolyte interface in supercapacitors.[8,9,17,25–29]

The success of the NMR approach stems from the unique capability to distinguish between ionic species that are confined inside the carbon nanopores (in-pore ions), and ions between the carbon particles and in the bulk electrolyte (ex-pore ions).[30,31] In the NMR spectra, in-pore ions give rise to resonances at lower chemical shift than the ex-pore ions, with the shift difference arising from the local magnetic field associated with the circulation of the delocalised carbon π electrons in the applied magnetic field.[32] The exact shift difference upon adsorption is nucleus-independent to a first approximation and depends primarily on the structure of the porous carbon, with the extent of structural ordering and the pore size both affecting the shift.[31–37]

Observation of resolved in-pore resonances in the NMR spectra of supercapacitor electrodes offers a large amount of valuable information; (i) the intensities of the in-pore resonances allow the number of in-pore anions and cations to be determined, and thus the composition of the carbon pores and supercapacitor charging mechanisms can be studied,[8,9,25–27] (ii) the chemical shift difference between in- and ex-pore resonances gives information about the carbon structure, with both carbon ordering and pore size distribution affecting the shift,[33–35] and (iii) the linewidth of the in-pore resonance can offer information about the dynamics of the in-pore ions.[25] However, in some experiments it can be difficult to resolve the in-pore resonances, which can limit the information that can be obtained. Examples include; *in situ* NMR experiments where there are intense signals from the large amount of free electrolyte in the cell and magic angle spinning is not possible,[8–10] experiments on carbons with small ring current shifts,[30,37] and experiments on viscous electrolytes where broad in-pore resonances are observed.[25] The development of advanced NMR methods that improve spectral resolution is therefore necessary if a wide range of electrolytes and carbon materials are to be studied.

We previously proposed that cross polarisation (CP) NMR experiments can be used to selectively observe in-pore ionic species in supercapacitor electrodes.[21] While CP is most commonly used as a signal enhancement method for dilute or insensitive nuclei, we took inspiration from studies of adsorption in zeolites,[38,39] and structural studies of biominerals,[40,41] where CP was used to "edit" the NMR spectra. Here, we show that it is possible to transfer magnetisation from the ^{13}C nuclear spins in carbide-derived carbon (CDC) electrodes to the nearby ^{1}H or ^{19}F nuclear spins of the in-pore cations and anions of 1-methyl-1-propylpyrrolidinium bis(trifluoromethanesulfonyl)imide ($Pyr_{13}TFSI$) ionic liquid. Studies of the CP kinetics as well as two-dimensional experiments confirm that in-pore ions are located within Ångströms of sp^2-hybridised carbon surfaces. In contrast, ex-pore ions are not detected in the CP experiments due to the much longer distances between these ions and the carbon surfaces and the faster dynamics of these free ions, making the CP technique a useful spectral editing method for studying adsorbed species in supercapacitor electrodes.

2. Experimental Details

2.1 Carbon Materials

^{13}C carbide-derived carbons were prepared from Ti^{13}C, which was first prepared by heating a mixture of ^{13}C powder (0.4 g, 99 at%, Sigma Aldrich) and crystalline titanium (1.7 g, ≥ 99.99 at%, Sigma Aldrich; particle size: 5 – 10 μm) at 1550 °C for 12 h (the heating rate was 10 K·min^{-1}) in flowing argon at atmospheric pressure. Following cooling to room temperature (10 K·min^{-1}), the resulting Ti^{13}C was ground by hand with an agate mortar to an average particle size between 2 and 50 μm. X-ray diffraction showed that this material is predominantly microcrystalline TiC, while a small fraction (< 1 wt%) graphitic carbon (i.e., non-reacted precursor material) was found via Rietveld refinement. To prepare Ti^{13}C-CDC-1000, the titanium was extracted by chlorine-treatment. Here, Ti^{13}C was flushed in argon for 30 min, and then heated (10 K·min^{-1}) to 1000 °C where this temperature was held for 3 h in flowing chlorine. The sample was then flushed with argon gas and treated in flowing hydrogen at 600°C for 3 h to remove residual chlorine and chloride species. After a final argon flushing, the resulting Ti^{13}C-CDC powder was cooled to room temperature. For preparing Ti^{13}C-CDC-800, the synthesis was identical, except that the chlorine-treatment temperature was 800 ºC. Further details can be found in our previous publication.[30]

All samples for NMR experiments were prepared using carbon films. These were fabricated using the standard method for preparing film electrodes, with a mixture of carbon powder (95 wt %) and polytetrafluoroethylene (PTFE) binder (5 wt %). More details on the electrode preparation can be found elsewhere.[30]

2.2 Ionic Liquids

1-Methyl-1-propylpyrrolidinium bis(trifluoromethanesulfonyl)imide ($Pyr_{13}TFSI$) ionic liquid (>98% purity, Tokyo Chemical Industry UK), was dried in vacuo for at least 48 h before preparing samples.

2.4 NMR Sample Preparation

For experiments on carbon film pieces (to which no potential has been applied) soaked with ionic liquid, samples were prepared as follows. Pieces of carbon film (between 2.4 and 4.3 mg) were cut out and dried for at least 15 h at 200 °C in vacuo before being transferred to an argon glovebox. These were packed into 2.5 mm outer diameter zirconia magic angle spinning (MAS) rotors, to which ~5 μL of $Pyr_{13}TFSI$ ionic liquid was added using a microsyringe.

2.4 NMR Experiments

NMR experiments were performed using a Bruker Avance spectrometer operating at a magnetic field strength of 7.1 T, corresponding to a ^{1}H Larmor frequency of 300.2 MHz. A Bruker 2.5 mm double resonance probe was used. Unless otherwise indicated, NMR experiments were performed at an MAS rate of 5 kHz. ^{19}F NMR spectra were referenced relative to neat hexafluorobenzene (C_6F_6) at −164.9 ppm, ^{1}H NMR spectra were referenced relative to tetramethylsilane using the CH_3 resonance of liquid ethanol at 1.2 ppm as a secondary reference, and ^{13}C NMR spectra were referenced to the resonance of the tertiary carbon atom in adamantane at 38.5 ppm. For direct excitation experiments, recycle delays were adjusted to give quantitative spectra for all nuclei. For CP experiments the recycle delay was 3 s in all cases.

The standard pulse sequence for CP[42] was modified by adding an initial "saturation train" of π/2 pulses on the channel on which data was acquired (see Supplementary Information, Figure S1). This was done to suppress artefacts arising from direct excitation, such that only signal generated by cross polarisation was observed. Unless otherwise stated, a train of 20 π/2 pulses was used, with the pulses separated by delays of 20 ms. The contact times for CP experiments are given in the figure captions. For CP experiments on Ti^{13}C-CDC-1000 samples, contact pulse powers of ~75 and ~70 kHz were used for ^{1}H and ^{13}C, respectively, with no power ramping applied to either channel. The same pulse powers were used for the spin-locking periods in the measurements of $T_{1\rho}$ (see below). For CP experiments on the Ti^{13}C-CDC-800 sample, contact pulses were ~60 kHz and ~50 kHz, for ^{13}C and ^{19}F respectively for the $^{13}C \rightarrow {}^{19}F$ experiments, while for $^{13}C \rightarrow {}^{1}H$, respective contact pulse powers were ~65 and ~50 kHz. Excitation pulse powers were between 95 and 122 kHz in all experiments. Spectral fits were carried out using the Sola package in Topspin software using a chemical shift anisotropy model. A single peak was used to fit the in-pore resonance, and a single peak was used for each ex-pore resonance. Sample temperatures were calibrated by ^{207}Pb NMR measurements on lead nitrate.[43]

3. Results and Discussion

Direct excitation and CP MAS NMR experiments are shown in Figure 1 for a sample of Ti^{13}C-CDC-800 (i.e. titanium carbide-derived carbon chlorine treated at 800ºC)[44] soaked with Pyr_{13}TFSI ionic liquid. This carbon was prepared from Ti^{13}C to provide a large number of spin active carbon atoms for magnetisation transfer (99% ^{13}C). The direct excitation experiment (*i.e.*, the normal, single resonance NMR experiment) reveals both in- and ex-pore resonances for the TFSI anions (Figure 1a), with the spectrum similar to that observed for YP50F activated carbon soaked with the same ionic liquid studied here.[25] The $^{13}C \rightarrow {}^{19}F$ CP experiment, on the other hand, reveals solely an in-pore resonance. Spectra with ^{1}H detection (Figure 1b) reveal similar effects for the Pyr_{13} cations,

with the $^{13}C \rightarrow {}^{1}H$ CP experiment showing only the in-pore cation resonances. The CP spectra allow for the reliable determination of in-pore peak positions and can assist the deconvolution of the direct excitation spectra.

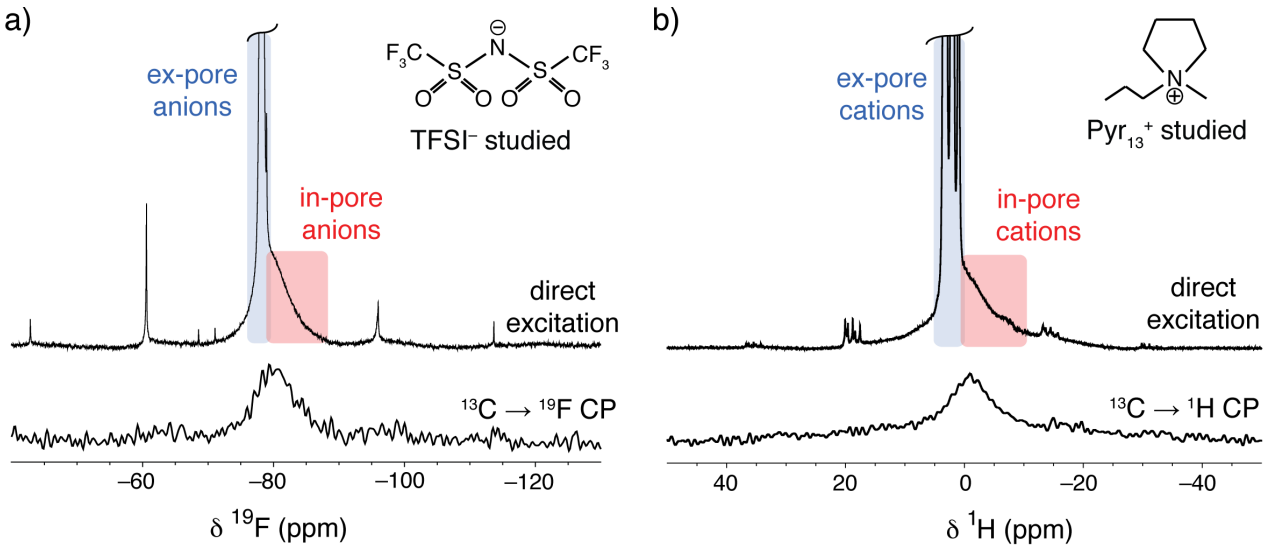

Figure 1 Room temperature (sample $T \sim 21$ ºC) ^{19}F (a) and ^{1}H (b) MAS NMR (7.1 T) spectra for Ti^{13}C-CDC-800 soaked with Pyr$_{13}$TFSI ionic liquid. In each case direct excitation and CP spectra (4 ms contact time) are shown. The CP experiments reveal solely the in-pore features. The signal-to-noise ratio is higher in the ^{1}H-detected CP experiment than the ^{19}F-detected experiment, despite the shorter experiment time for the former (~15 minutes vs. ~2 hours), see below. The CP experiments take considerably longer than the direct excitation experiments, for which the total experiment time is on the order of 1 minute in each case. The sample spinning speed is 5 kHz.

The selective detection of in-pore resonances in the CP experiments may be rationalised, given that magnetisation transfer in the CP experiment occurs via heteronuclear dipolar couplings. Firstly, the strength of the dipolar couplings are proportional to r^{-3}, where r is the distance between the coupled nuclei.[45] Thus, only spins separated by a few Ångströms are detected in the CP experiments. Secondly, the heteronuclear dipolar couplings are averaged by molecular motion, such that any couplings present for ex-pore ions will be averaged to zero by isotropic tumbling. In contrast, in-pore ions in organic electrolytes have been measured to have mobilities that are orders of magnitude slower than those observed in the free electrolyte,[17] and further reductions of in-pore mobility are expected for the pure ionic liquid studied here.[25] Furthermore, the confined spaces within the anisotropic pores means that even in the presence of ionic motion, residual dipolar couplings between the ions and the carbon surface will remain, albeit orders of magnitude smaller than those observed in rigid systems. Together these effects explain why only the in-pore resonances are detected in the CP experiments.

The CP experiments offer a method to "edit" the spectra, though it is noted that they take considerably longer than direct excitation experiments, with the ^{19}F- and ^{1}H-detected CP

experiments in Figure 1 taking ~2 hours and ~15 minutes to acquire, respectively, compared to experiment times of ~1 minute for each of the direct excitation experiments. The inefficiency of the CP experiments is in part ascribed to the reduced dipolar couplings due to the residual motion, but it is explored in more detail in the next sections. The ^{1}H-detected CP measurements (cations) offer better signal-to-noise ratios than the ^{19}F-detected measurements (anions). This arises in part as there are more hydrogen atoms per cation than there are fluorines per anion, but may also reflect differences in the dynamics of the $TFSI^{-}$ anions and the Pyr_{13}^{+} cations. For example, all of the fluorine atoms belong to $–CF_3$ groups and are expected to have considerable rotational dynamics.

The CP transfer is performed in reverse to the conventional sense here. Typically CP is used to enhance signal intensity for insensitive nuclei (*e.g.*, ^{13}C), by transferring magnetisation from sensitive nuclei (such as ^{1}H or ^{19}F), with the maximum theoretical enhancement given by the ratio of the gyromagnetic ratios of the nuclei (*e.g.*, a maximum enhancement of ~4 for $^{1}H \rightarrow {}^{13}C$).[45] Here, however, by transferring from an insensitive nucleus (^{13}C) to a sensitive nucleus (such as ^{1}H), a signal diminishment by a factor of ~4 is expected. The more sensitive nuclei usually have the added benefit of shorter longitudinal relaxation times (T_1) allowing a faster repetition of the pulse sequence when carrying out the CP transfer in the conventional direction. The success of the reverse approach carried out here relies on the isotopic enrichment of the carbon electrode (99 % ^{13}C), which provides more magnetisation to transfer, while also giving rise to relatively short T_1s for ^{13}C in the solid state. For example, the T_1 value of Ti^{13}C-CDC-1000 was measured as 0.9 s by the saturation recovery method.

^{1}H NMR spectra for Ti^{13}C-CDC-1000 soaked with Pyr_{13}TFSI ionic liquid reveal similar effects to those for Ti^{13}C-CDC-800 (Figure 2a), with the CP spectra shown for two different MAS rates here. The 2D heteronuclear correlation (HETCOR) experiment shown in Figure 2b confirms that the sp^2-hybridised carbon surface (δ ^{13}C = 124 ppm) transfers magnetisation to the in-pore cations (δ ^{1}H = –1.1 ppm) in the CP experiment. No correlations are seen for the directly bonded ^{13}C-^{1}H pairs in the Pyr_{13}^{+} cations. This is largely because the carbon nuclei in the cations have the natural abundance of ^{13}C spins (~1 %), such that there are very few ^{13}C nuclei to transfer magnetisation from. Moreover, rotation of the in-pore cations will average the orientation of the intramolecular ^{13}C-^{1}H vectors (with respect to the applied magnetic field direction), which will average the intramolecular dipole-dipole couplings to zero in the limit of isotropic rotation. The remaining ^{13}C-^{1}H dipolar couplings are between the ^{13}C spins in the porous carbon and the ^{1}H spins in the cations. Intermolecular ^{13}C-^{1}H dipolar couplings will still exist between the cations, but these couplings will be severely reduced by the translational and rotational motion of the cations, as such motion will vary the orientations and lengths of the ^{13}C-^{1}H inter-nuclear vectors.

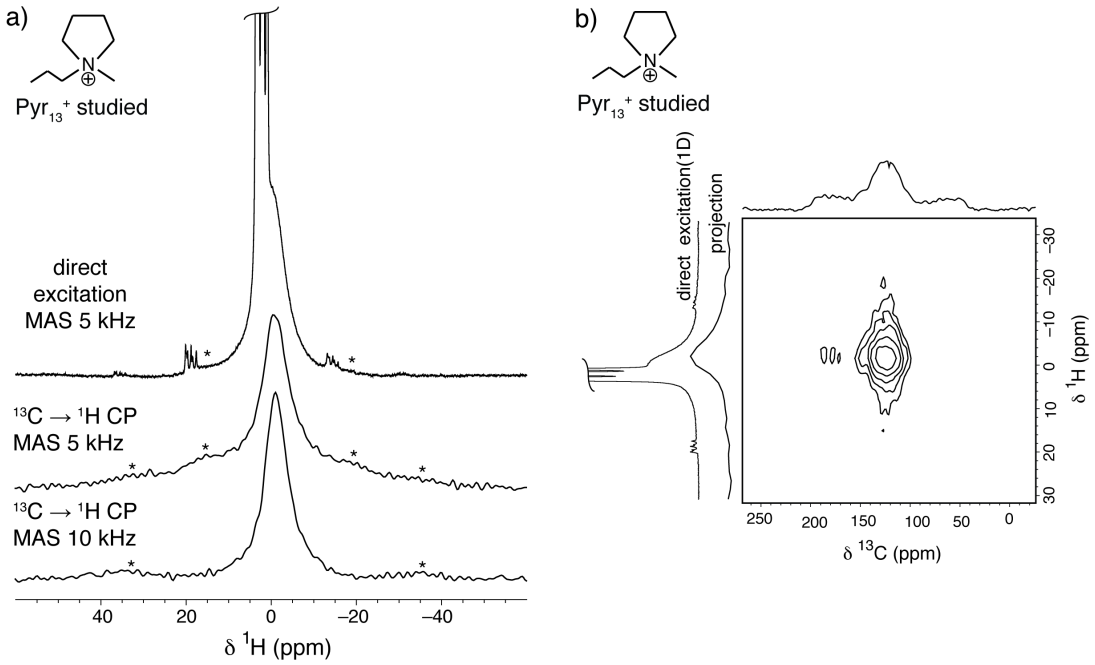

Figure 2 Room temperature (sample T ~21 ºC) NMR (7.1 T) spectra for Ti^{13}C-CDC-1000 soaked with Pyr$_{13}$TFSI ionic liquid. (a) ^{1}H NMR direct excitation and CP experiments, with the sample spinning speeds indicated on the figure, and in-pore spinning sidebands marked with asterisks. (b) ^{13}C → ^{1}H 2D HETCOR experiment (5 kHz MAS). The contact time for CP was 6 ms in all cases.

Interestingly the CP spectra (Figure 2a) show more intense in-pore spinning sidebands than the direct excitation spectrum, where these sidebands are barely visible. This was quantified by spectral fits (Sola program in Topspin) that give a measure of the width, W_{aniso}, of the spinning sideband pattern (the W_{aniso} parameter is analogous to a chemical shift anisotropy parameter, Δ_{aniso}). For the in-pore resonance here, W_{aniso} was found to be 5, 20 and 24 ppm for the direct excitation (MAS 5 kHz), CP (MAS 5 kHz) and CP (MAS 10 kHz) experiments, respectively, with the values for the two CP spectra agreeing within the estimated error associated with the fits (~2 or 3 ppm). The spectral fits also reveal that the linewidth of the isotropic in-pore resonance is larger in the CP (MAS 5 kHz) spectrum than in the direct excitation spectrum at the same sample spinning speed, with full-linewidths at half-maximum intensity (FWHMs) of 2500 and 2000 Hz, respectively. Together these findings suggest that the CP experiments detect a subset of the in-pore ions with slower dynamics. It is hypothesised that the CP experiments favour the most confined ions that are undergoing the slowest translational and rotational motion and therefore have the largest residual dipolar couplings.

Additional structural and dynamical information can be obtained from CP experiments by examining the kinetics of the magnetisation transfer process.[46] CP experiments were repeated with different contact times (the time during which magnetisation is transferred) and the build-up (and decay) of the signal intensity was measured. ^{13}C → ^{1}H CP kinetics for measurements on Ti^{13}C-

CDC-1000 soaked with $Pyr_{13}TFSI$ show that the signal intensity builds up as the contact time is increased to about 6 ms, after which slight decreases in signal intensity are observed (Figure 3a). Following the approach reviewed by Kolodziejski and Klinowski,[46] the build-up of the signal can be fit according to:

$$I(t) = A\left[\exp\left(\frac{-t}{T_{1\rho}(^{13}C)}\right) - \exp\left(-t\left(\frac{1}{T_{CP}} + \frac{1}{T_{1\rho}(^{1}H)}\right)\right)\right] \qquad \text{[Equation 1]}$$

Where t is the contact time, T_{CP} is a time constant associated with the magnetisation transfer from ^{1}H to ^{13}C, $T_{1\rho}(^{13}C)$ and $T_{1\rho}(^{1}H)$ are longitudinal relaxation times in the rotating frame, and A is a constant given by:

$$A = I_0\left(1 + \frac{T_{CP}}{T_{1\rho}(^{1}H)} - \frac{T_{CP}}{T_{1\rho}(^{13}C)}\right)^{-1} \qquad \text{[Equation 2]}$$

Where I_0 is a constant that is proportional to the signal intensity that would be obtained in a direct excitation experiment for the species that undergo cross polarisation.[46]

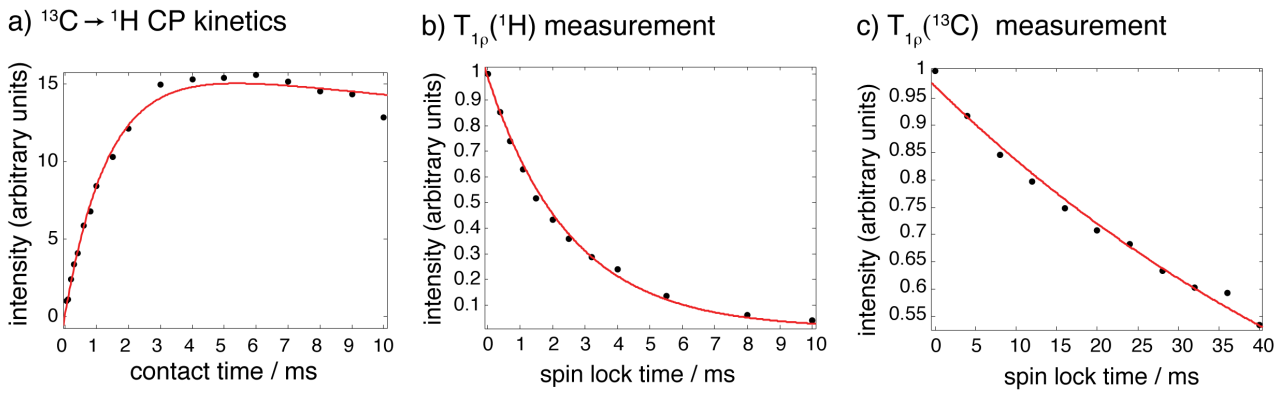

Figure 3 CP kinetics for $Ti^{13}C$-CDC-1000 soaked with $Pyr_{13}TFSI$ ionic liquid (5 kHz MAS, sample temperature ~21 ºC). (a) $^{13}C \rightarrow {}^{1}H$ CP kinetics with a fit to Equation 1 shown in red. (b), (c) show relaxation measurements for $T_{1\rho}(^{1}H)$ and $T_{1\rho}(^{13}C)$, respectively, with exponential fits of the form $S_0\exp(-\tau/T_{1\rho})$ shown, where τ is the spin lock time, and S_0 is the signal for $\tau = 0$.

The relaxation times $T_{1\rho}(^{13}C)$ and $T_{1\rho}(^{1}H)$ were independently measured as 67 (6) and 2.5 (0.2) ms, respectively, by carrying out separate spin-locking experiments (Figure 3b,c). These parameters were fixed in the fit of the CP kinetics to Equation 1 (Figure 3a), where a value of 3.0 (0.7) ms was obtained for T_{CP}. Similar results were obtained for a second independent $Ti^{13}C$-CDC-1000 sample soaked with the same ionic liquid, with a slightly shorter T_{CP} value of 2.1 (0.3) ms obtained (Figure S2, Supplementary Information). While the fits are generally good, there is some deviation between the fitted function and the experimental data at contact times above 3 ms (Figure 3a, Figure S2a),

indicating that there may be a distribution of different in-pore ^{1}H environments, each with slightly different T_{CP} and $T_{1\rho}$ values. This may arise from the different in-pore CH_3 and CH_2 Pyr_{13}^{+} resonances that are unresolved in the NMR spectra, but which are expected to exhibit different dynamics.

The T_{CP} value depends on the strength of the dipolar couplings, with shorter values corresponding to stronger dipolar couplings. T_{CP} therefore depends on both; the distances between the coupling spins, and the presence of any motion of these spins relative to each other.[47,48] The relatively long T_{CP} values of 3.0 (0.7) and 2.1 (0.3) ms obtained here are consistent with an intermolecular interaction between the carbon surface and the protons on the in-pore Pyr_{13} cations. Relatively long T_{CP} times are typical for systems with relatively large ^{13}C-^{1}H distances and/or considerable dynamics. For example, in solid adamantane the rapid molecular motion of the molecules on the crystal lattice averages out the intramolecular dipole-dipole couplings with magnetisation transfer then occurring via the longer range intermolecular couplings with a T_{CP} value of ~ 2.3 ms.[47,48] This is in stark contrast to the short intramolecular T_{CP} values of ~ 0.1 - 0.5 ms measured for carbons with directly bonded protons in typical organic solids,[49] and is more similar to the longer (again intramolecular) T_{CP} times of 0.5 - 2 ms obtained for carbons with no directly bonded protons.[50] Interestingly, very long intermolecular T_{CP} values have been measured for the fullerene-toluene mixtures studied by Kolodziejski *et al.*, where T_{CP} was measured as 13 ms for magnetisation transfer from the fullerenes to protons in toluene solvent).[51] In our case it is probable that both relatively long carbon-ion distances (of order 5 Å), and ionic translation and rotation, contribute to the long measured T_{CP} value. Indeed, initial variable temperature measurements indicate a more gradual build-up of CP signal intensity at an elevated temperature of 60 ºC (Supplementary Information, Figure S3), due to the faster in-pore ion dynamics at this temperature.

4. Conclusions

In summary, we have demonstrated the application of CP NMR as a method to selectively observe in-pore ions in supercapacitor electrode materials wetted with ionic liquid. When magnetisation is transferred from ^{13}C in Ti^{13}C-CDCs to nuclei in the cations (^{1}H) or anions (^{19}F), only the in-pore resonances are observed. Together with two-dimensional NMR and CP kinetics, our results confirm that in-pore ions are located within Ångström distances of the carbon surfaces, while ex-pore ions are more remote. In practice, the CP experiments select a subset of the in-pore ions, with only the most confined ions observed. Our work demonstrates that heteronuclear correlations can aid with the selective observation of charge storing ions for supercapacitor systems where spectral resolution is limited, such as *in situ* studies. Initial attempts at static *in situ* CP measurements on supercapacitors have been carried in our laboratory, though we have observed unwanted electrolyte

heating effects associated with the long RF pulses used in CP experiments and the presence of highly ionic electrolyte solutions. Further attempts at these experiments should mitigate sample heating by a combination of low power RF pulses and appropriate cooling gases. In future, the CP approach may also offer detailed information on the rotational and translational dynamics of confined ions, though for this to be realised, our experimental measurements of CP kinetics must be coupled with molecular simulations. Beyond heteronuclear NMR experiments, relaxometry or diffusometry may also offer effective methods for spectral editing, and these will be explored in future work.

Supplementary Information Available

Details of pre-saturation used for CP experiments and additional CP kinetics data.

Acknowledgements

A.C.F., J.M.G., and C.P.G. acknowledge the Sims Scholarship (A.C.F.), EPSRC (via the Supergen consortium, J.M.G.), and the EU ERC (via an Advanced Fellowship to C.P.G.) for funding. A.C.F. and J.M.G. thank the NanoDTC Cambridge for travel funding. Yury Gogotsi and Volker Presser are thanked for stimulating discussions and for synthesising Ti^{13}C-CDC samples and carrying out initial characterization at Drexel University. Céline Merlet is thanked for stimulating discussions.

References

1. M. Salanne, B. Rotenberg, K. Naoi, K. Kaneko, P.-L. Taberna, C. P. Grey, B. Dunn, and P. Simon, *Nat. Energy*, 2016, **1**, 16070.
2. A. C. Forse, C. M. Merlet, J. M. Griffin, and C. P. Grey, *J. Am. Chem. Soc.*, 2016, **138**, 5731–5744.
3. C. Merlet, B. Rotenberg, P. A. Madden, P.-L. Taberna, P. Simon, Y. Gogotsi, and M. Salanne, *Nat. Mater.*, 2012, **11**, 306–310.
4. C. Merlet, C. Péan, B. Rotenberg, P. A. Madden, B. Daffos, P.-L. Taberna, P. Simon, and M. Salanne, *Nat. Comm.*, 2013, **4**, 2701.
5. S. Kondrat, P. Wu, R. Qiao, and A. A. Kornyshev, *Nat. Mater.*, 2014, **13**, 387–393.
6. J. Vatamanu, M. Vatamanu, and D. Bedrov, *ACS Nano*, 2015, 5999–6017.
7. J. Vatamanu, Z. Hu, D. Bedrov, C. Perez, and Y. Gogotsi, *J. Phys. Chem. Lett.*, 2013, **4**, 2829–2837.
8. J. M. Griffin, A. C. Forse, W.-Y. Tsai, P.-L. Taberna, P. Simon, and C. P. Grey, *Nat. Mater.*, 2015, **14**, 812–819.

9. J. M. Griffin, A. C. Forse, H. Wang, N. M. Trease, P. Simon, and C. P. Grey, *Faraday Disc.*, 2014, **176**, 49–68.
10. H. Wang, A. C. Forse, J. M. Griffin, N. M. Trease, L. Trognko, P.-L. Taberna, P. Simon, and C. P. Grey, *J. Am. Chem. Soc.*, 2013, **135**, 18968–80.
11. F. W. Richey, C. Tran, V. Kalra, and Y. A. Elabd, *J. Phys. Chem. C*, 2014, **118**, 21846–21855j.
12. M. D. Levi, G. Salitra, N. Levy, D. Aurbach, and J. Maier, *Nat. Mater.*, 2009, **8**, 872–875.
13. W.-Y. Tsai, P.-L. Taberna, and P. Simon, *J. Am. Chem. Soc.*, 2014, **136**, 8722–8728.
14. C. Prehal, D. Weingarth, E. Perre, R. T. Lechner, H. Amenitsch, O. Paris, and V. Presser, *Energy Environ. Sci.*, 2015, **8**, 1725–1735.
15. S. Boukhalfa, L. He, Y. B. Melnichenko, and G. Yushin, *Angew. Chem. Int. Ed.*, 2013, **52**, 1–6.
16. S. Boukhalfa, D. Gordon, L. He, Y. B. Melnichenko, N. Nitta, A. Magasinski, and G. Yushin, *ACS Nano*, 2014, **8**, 2495–2503.
17. A. C. Forse, J. M. Griffin, C. Merlet, J. Carretero-Gonzalez, A.-R. O. Raji, N. M. Trease, and C. P. Grey, *Nat. Energy*, 2017, **2**, 16216.
18. C. Prehal, C. Koczwara, N. Jackel, A. Schreiber, M. Burian, H. Amenitsch, M. A. Hartmann, V. Presser, and O. Paris, *Nat. Energy*, 2017, 16215.
19. R. Futamura, T. Iiyama, Y. Takasaki, Y. Gogotsi, M. J. Biggs, M. Salanne, J. Ségalini, P. Simon, and K. Kaneko, *Nat. Mater.*, 2017, DOI: 10.1038/NMAT4974.
20. Z.-X. Luo, Y.-Z. Xing, S. Liu, Y.-C. Ling, A. Kleinhammes, and Y. Wu, *J. Phys. Chem. Lett.*, 2015, **6**, 5022–5026.
21. F. W. Richey, B. Dyatkin, Y. Gogotsi, and Y. A. Elabd, *J. Am. Chem. Soc.*, 2013, **135**, 12818–12826.
22. C. Pean, B. Daffos, B. Rotenberg, P. Levitz, M. Haefele, P.-L. Taberna, P. Simon, and M. Salanne, *J. Am. Chem. Soc.*, 2015, **137**, 12627–32.
23. C. Péan, C. Merlet, B. Rotenberg, P. A. Madden, P.-L. Taberna, B. Daffos, M. Salanne, and P. Simon, *ACS Nano*, 2014, **8**, 1576–1583.
24. Y. He, J. Huang, B. G. Sumpter, A. A. Kornyshev, and R. Qiao, *J. Phys. Chem. Lett.*, 2015, **6**, 22–30.
25. A. C. Forse, J. M. Griffin, C. Merlet, P. M. Bayley, H. Wang, P. Simon, and C. P. Grey, *J. Am. Chem. Soc.*, 2015, **137**, 7231–7242.
26. M. Deschamps, E. Gilbert, P. Azais, E. Raymundo-Piñero, M. R. Ammar, P. Simon, D. Massiot, and F. Béguin, *Nat. Mater.*, 2013, **12**, 351–358.
27. Z.-X. Luo, Y.-Z. Xing, Y.-C. Ling, A. Kleinhammes, and Y. Wu, *Nat. Comm.*, 2015, **6**,

6358.
28. A. Ilott, N. Trease, C. Grey, and A. Jerschow, *Nat. Comm.*, 2014, **5**, 4536.
29. J. M. Griffin, A. C. Forse, and C. P. Grey, *Solid State Nucl. Magn. Reson.*, 2016, **74**, 16–35.
30. A. C. Forse, J. M. Griffin, H. Wang, N. M. Trease, V. Presser, Y. Gogotsi, P. Simon, and C. P. Grey, *Phys. Chem. Chem. Phys.*, 2013, **15**, 7722–7730.
31. L. Borchardt, M. Oschatz, S. Paasch, S. Kaskel, and E. Brunner, *Phys. Chem. Chem. Phys.*, 2013, **15**, 15177–84.
32. A. C. Forse, J. M. Griffin, V. Presser, Y. Gogotsi, and C. P. Grey, *J. Phys. Chem. C*, 2014, **118**, 7508–7514.
33. C. Merlet, A. C. Forse, J. M. Griffin, D. Frenkel, and C. P. Grey, *J. Chem. Phys.*, 2015, **142**, 94701.
34. A. C. Forse, C. Merlet, P. K. Allan, E. K. Humphreys, J. M. Griffin, M. Aslan, M. Zeiger, V. Presser, Y. Gogotsi, and C. P. Grey, *Chem. Mater.*, 2015, **27**, 6848–6857.
35. Y.-Z. Xing, Z.-X. Luo, A. Kleinhammes, and Y. Wu, *Carbon N. Y.*, 2014, **77**, 1132–1139.
36. Y. Xu, T. Watermann, H.-H. Limbach, T. Gutmann, D. Sebastiani, and G. Buntkowsky, *Phys. Chem. Chem. Phys.*, 2014, **16**, 9327–9336.
37. R. J. Anderson, T. P. McNicholas, A. Kleinhammes, A. Wang, J. Liu, and Y. Wu, *J. Am. Chem. Soc.*, 2010, **132**, 8618–8626.
38. K. H. Lim and C. P. Grey, *Chem. Commun.*, 2000, **13**, 2257–2258.
39. J. L. White, L. W. Beck, and J. F. Haw, *J. Am. Chem. Soc.*, 1992, **114**, 6182–6189.
40. J. Kolmas and W. Kolodziejski, *Chem. Commun.*, 2007, **21**, 4390–4392.
41. J. Kolmas and W. Kolodziejski, *Chem. Phys. Lett.*, 2012, **554**, 128–132.
42. D. C. Apperley, R. K. Harris, and Paul Hodgkinson, *Solid-state NMR Basic Principles and Practice*, 2012.
43. P. A. Beckmann and C. Dybowski, *J. Magn. Reson.*, 2000, **146**, 379–380.
44. V. Presser, M. Heon, and Y. Gogotsi, *Adv. Funct. Mater.*, 2011, **21**, 810–833.
45. D. P. Burum, *Encycl. Nucl. Magn. Reson.*, 1996, **3**, 1535–1542.
46. W. Kolodziejski and J. Klinowski, *Chem. Rev.*, 2002, **102**, 613–628.
47. A. Pines, M. G. Gibby, and J. S. Waugh, *J. Chem. Phys.*, 1973, **59**, 569.
48. D. G. Rethwisch, M. A. Jacintha, and C. R. Dybowski, *Anal. Chim. Acta.*, 1993, **283**, 1033–1043.
49. L. B. Alemany, D. M. Grant, R. J. Pugmire, T. D. Alger, and K. W. Zilm, *J. Am. Chem. Soc.*, 1983, 2133–2141.
50. L. B. Alemany, D. M. Grant, R. J. Pugmire, T. D. Alger, and K. W. Zilm, *J. Am. Chem. Soc.*, 1983, 2142–2147.

51. W. Kolodziejski, A. Corma, K. Wozniak, and J. Klinowski, *J. Phys. Chem.*, 1996, **100**, 7345–7351.